Tunneling FET With Embedded P^+ Pocket as a High Sensitivity Biosensor for Label-Free Detection

Milad Azarkerdar [1] and Ali Naderi*[2]

***Abstract*-- In this paper, an efficient structure for tunneling field effect transistors (TFETs) with P^+ pocket is proposed for label-free detection of biomolecules. This structure includes a double gate TFET with $P^+P^-N^+$ doping profile for source, channel, and drain regions and an embedded P^+ pocket in the channel to control the band-to-band tunneling (BTBT). The biomolecules are captured in the cavity region and affect the band bending. The capacitive behavior of biomolecules causes further band bending where their dielectric constant is increased. The presence of P^+ pocket at the source side of TFET causes more changes in the capacitive behavior and in current and consequently increases the sensitivity. For the detection of the biomolecule with K=4, the proposed structure shows more than 60% improvement in sensitivity. It enhances the sensitivity for all investigated dielectric constants, where the enhancement is more considerable for biomolecules with higher dielectric constants. For more evaluation, the biosensor is assessed in different widths and impurity densities of P^+ region. It demonstrates that the proposed structure can efficiently tolerate the variations in physical dimension and impurity concentration while it maintains higher sensitivities.**

***Index Terms*- Tunneling FET, Biomolecule, Sensitivity, Band-to-Band Tunneling, Band Bending.**

I. Introduction

IN recent years, biosensors have been considered one of the main devices in many biological, medical, and industrial applications such as security and inspection, food processing, drug delivery, early-stage recognition and analysis of diseases, environment protection, etc. In biosensors, biological elements are used for the detection mechanism, including microorganisms, antibodies, biological tissues, proteins, enzymes, and drugs. The detection of biomolecules in a short time with high sensitivity and reliability is the main aim in designing modified structures of biosensors.

The field effect transistors (FETs) based on electrochemical biosensors attract a lot of research interest because of their benefits in label-free detection, compatibility with the standard CMOS technology, their small dimensions, prevalent manufacturing methods, and their acceptable cost in mass production. The electrical properties of FETs, such as ON current, off current, current ratio, ambipolar behavior, and subthreshold swing (SS), may experience variations in the existence of biomolecules. These variations are used to detect the biomolecules. Due to the electronic physics limitation on SS from kT/q coefficient, for the biosensors based on FETs, the SS cannot be less than 60 mV/decade, where it consequently limits the reduction in response time. To remove this limitation on SS, tunnel-based devices are employed [1-4]. The sensitivity and response time are enhanced where conventional FETs are replaced by tunnel FETs (TFETs) to detect biomolecules [5-9]. Nevertheless, while the weakness of the tunneling device is in its small ON current, this subject is not a severe limitation for TFETs in biosensor requirements [3, 5].

The TFET biosensors based on the Dielectric-modulated (DM) concept have a significant portion for label-free distinguishing of molecules. The gate oxide capacitance shows some variations in the presence of biomolecules. These variations are a result of the dielectric constant or charge density changes from the presence of biomolecules in the nanogap region that is formed in the gate insulator region or the gate metal [10, 11]. Due to the proven efficiency of TFETs as biosensors, different methods and structures have been explored and suggested with the aim of more improvement in the sensing ability of TFETs and to reduce their limitations.

The works, such as those in [12, 13], investigated the TFET biosensors generally, and the other, such as those in [14-24], focused on specific structures. The dual channel trench [14], Ion sensitive structure [15], gate underlap and overlap [16], hetero-structures [17, 24], double gate [18] and short gate configuration [21], using different materials like carbon nanotube [19], working on vertical structure [20], junction-less [22] and doping-less concepts [23] are among recently reported works. Some of the other recently reported works have concentrated on a mixture of multi techniques to improve the device performance efficiently [25-29]. Using different ideas from different technologies is the basis of these structures to enhance the parameters. Briefly, due to the increasing demands for biosensors, researchers will propose more structures and configurations for TFETs.

In this paper, a dielectrically modulated structure with P^+ pocket is proposed to enhance the performance of TFETs as label-free biosensors. The ON current and the OFF current are used to investigate the ability of the proposed structure. The

1. Electrical Engineering Department, Energy Faculty, Kermanshah University of Technology, Kermanshah, Iran.
2. Electrical Engineering Department, Engineering Faculty, Imam Khomeini International University, Qazvin, Iran.

*Corresponding author Email: a.naderi@eng.ikiu.ac.ir

consequences show that the P^+ embedded device is an efficient biosensor in terms of investigated parameters.

The text body of this paper is arranged as follows: Section II defines the proposed structure specifications and simulation details. In section III, simulation results and discussions are presented. In the last part, this paper is concluded in part IV.

II. Biosensor Architecture and Simulation Conditions

Fig. 1 illustrates a 2-D schematic for the basic and proposed structures. Both structures are double gate architecture, which use $P^+P^-N^+$ doping profile for source, channel, and drain sections, respectively. The cavities are embedded in structures, as seen in the figure. The cavity is fixed neighboring the device tunneling junction to immobilize targeted biomolecules. The cavity shaped in the device structure can be created by etching the oxide of gate entirely, and the exposed Si region would then be isolated by an oxide layer resulting from an oxidation process [25]. Device dimensions, doping concentration, and related parameters are mentioned in Table I. Both structures are the same except in P^+ region located in the source to channel junction under the gate for the proposed structure. The object of locating a cavity only at the source side is the mechanism of current conduction of tunneling FETs, which is principally a junction phenomenon. A sharp turn on is a result of proper gate voltage coupling in a slight region next to the tunneling junction.

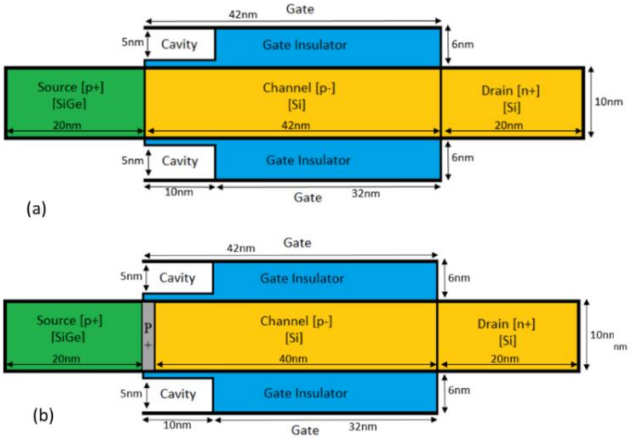

Fig. 1. Illustration of (a) conventional and (b) proposed TFET-based biosensors. The difference between structures is in the P^+ region embedded in the proposed biosensor with 2 nm width and 10 nm height.

Numerical simulation is done by ATLAS from SILVACO, where the basis for device simulation is provided by coupling the diffusion and continuity equations [30, 31, 32]. The important issue in simulation is band-to-band tunneling (BTBT) phenomena. In this study, the nonlocal BTBT model accessible in ATLAS is calibrated with experimental data presented for P-N-P-N tunneling FET [25]. Activating the proper models in the simulator have been considered to take the required phenomena into account, including field-dependent mobility model, the Auger model, the Shockley-Hall-Read (SHR), and Fermi–Dirac statistics to consider the degeneration/recombination, band gap narrowing, and the quantum confinement model to consider quantum tunneling. To obtain the reliable output, the simulator is calibrated with experimental data as shown in Fig. 2. A good agreement between double gate P-N-P-N tunneling FET and its real data [25] is observed. This calibration is used for simulating our proposed structure and its conventional counterpart.

TABLE I
The Dimensions and Impurity Values to Simulate the Mentioned Biosensors

Parameter	Value
Gate length	42 nm
Source length	20 nm
Drain length	20 nm
Channel width	10 nm
Gate width	6 nm
Drain impurity (n^+)	5×10^{19} cm^{-3}
Source impurity (p^+)	5×10^{19} cm^{-3}
Channel impurity (p^-)	1×10^{12} cm^{-3}
Length of Cavity	10 nm
Width of Cavity	5 nm
width of P^+ region	2 nm
Height of P^+ region	10 nm
Impurity of P^+ region	5×10^{19} cm^{-3}

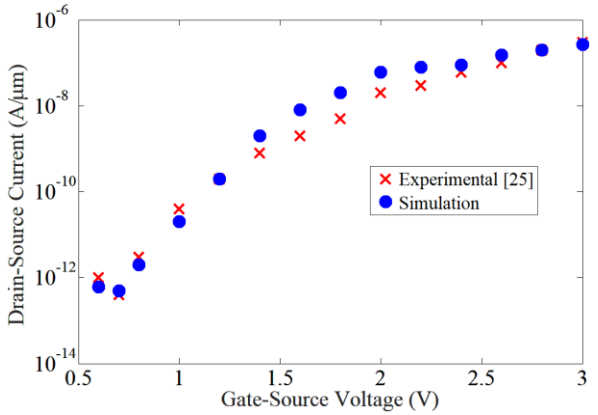

Fig. 2. The experimental data [25] to calibrate the simulator and the outputs of the simulator after calibration.

III. Results and Discussions

The biomolecules can be categorized into neutral and charged groups. In this paper, we considered the detection of neutral biomolecules. The dielectric constant change in the cavity region is used for the analysis of drain current and other characteristics of neutral biomolecules. When there is no biomolecule in the cavity region, its dielectric constant is K=1. Once the biomolecules are accumulated in the cavity region, the dielectric constant of the cavity is increased, and the gate capacitance increases accordingly. This leads to making the drain current and other parameters experience enough changes to be used as detection parameters for sensing the biomolecules and their related materials. They have permittivity larger than K=1, for instance, streptavidin = 2.1, APTES = 3.57, uricase = 1.54, biotin=2.63, protein = 2.5, cellulose= 6.1, DNA= 8.7 and so on [33, 34, 35] where K = 1 shows that cavity is occupied

with air. At V_{GS}=1 V, the I_{DS}-V_{DS} characteristics of basic and proposed structures are illustrated in Fig. 3 for different biomolecules with various dielectric constants from K=1 to 11. It can be seen that the proposed structure results in higher current capability, especially for biomolecules with a higher dielectric constant. It is worth mentioning that the difference between structures is more observable by an increase in the dielectric constant.

The FET current directly depends on the device oxide capacitance. The more oxide dielectric, the more oxide capacitance and the higher device current. In other point of view, by increasing the dielectric constant, the threshold voltage decreases and the saturation current rises. Furthermore, the existence of the P^+ region amplifies the BTBT for the proposed biosensor, and consequently it offers better current characteristics than its conventional counterpart.

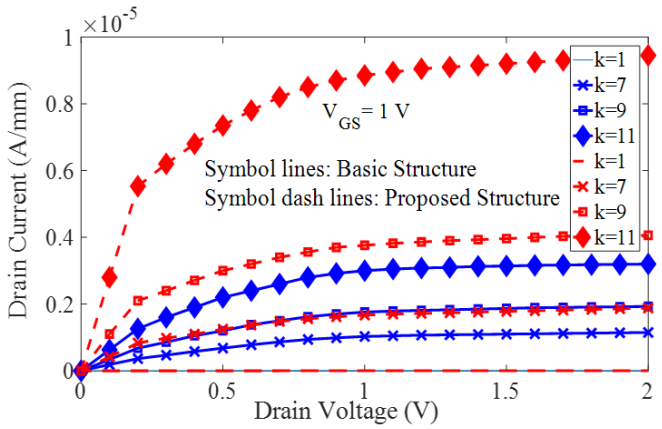

Fig. 3. Current-voltage characteristics of the proposed and basic structures where different materials with different dielectric constant are in cavity region.

For more investigation Fig.s 4 (a), and (b) are illustrated for materials with various dielectric constants in cavity section where drain source voltage is fixed at 0.25 V. The difference between both structures is more apparent in higher gate voltages. When the biomolecules are gathered in cavity region, the dielectric constant of the cavity is amplified, and the gate capacitance increases consequently.

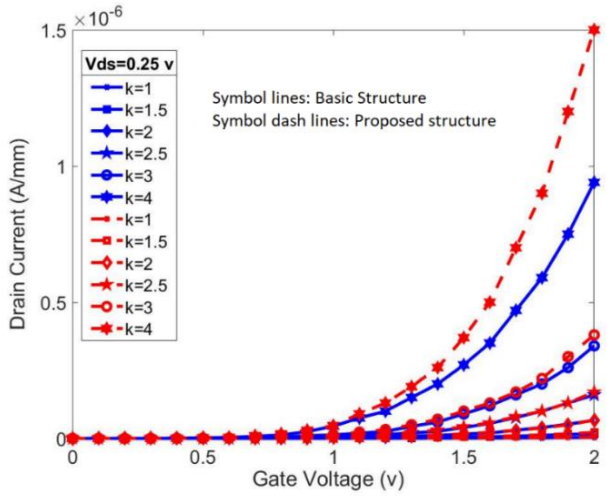

(a)

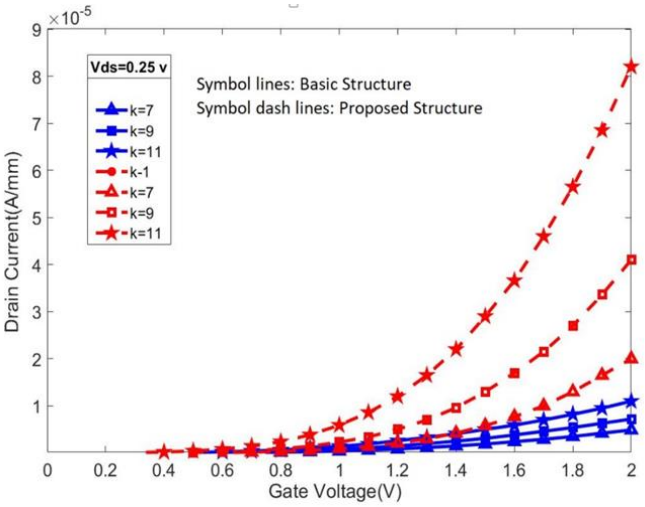

(b)

Fig. 4. Drain current versus gate voltage graph at V_{DS}=0.25 V for proposed and basic structures where different materials with various dielectric constant are accumulated in cavity section.

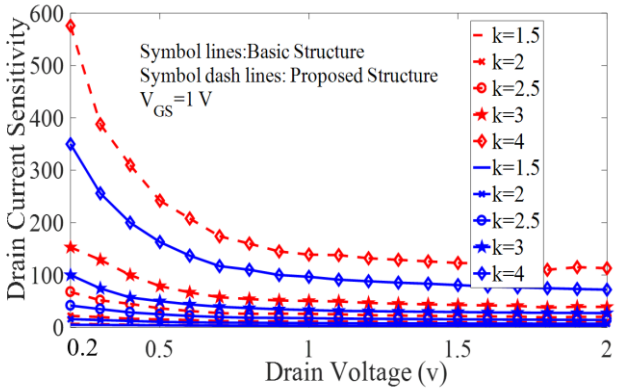

(a)

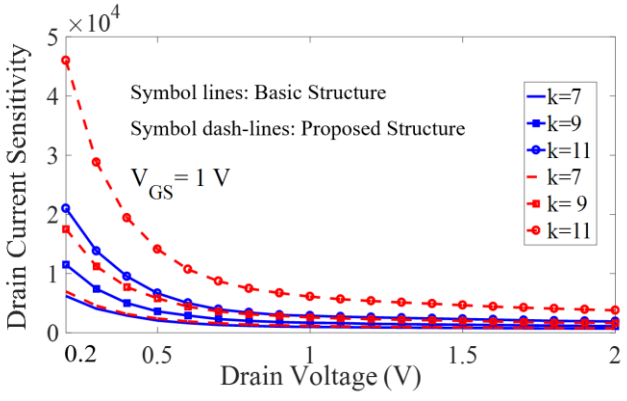

(b)

Fig. 5. Sensitivity of conventional and proposed structures at different drain-source voltage where gate-source voltage is fixed at 1 V.

A sensitivity investigation is done to distinguish the variation of goal biomolecules regarding air on electrical characteristics. Typically, higher sensitivity is desired, as it reveals a high possibility to sense goal biomolecules [10]. In the case of tunnel FETs, the current sensitivity is calculated using the bellow equation:

$$Sensitivity_{I-DS} = S_{I-DS} = \frac{I_{DS-Bio} - I_{DS-Air}}{I_{DS-Air}} \quad (1)$$

In which $I_{I-DS-Air}$ and $I_{I-DS-Bio}$ are the drain-source current for the conditions where the cavity is occupied with air and biomolecules, correspondingly [10, 11, 22]. For other parameters such as OFF current, the biosensor sensitivity is formulated similarly by observing the variation of the parameter for air and

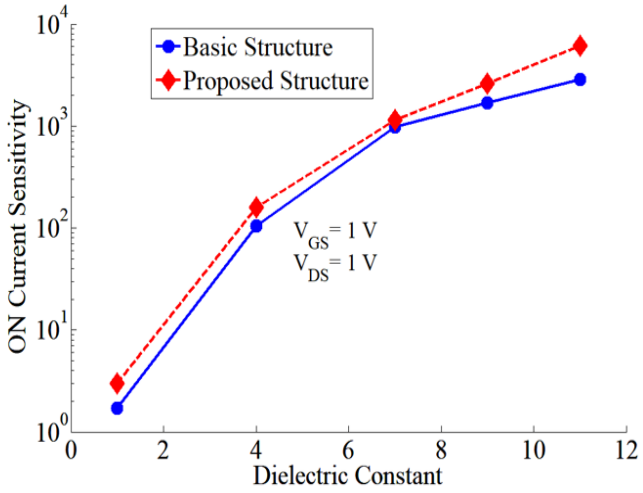

(a)

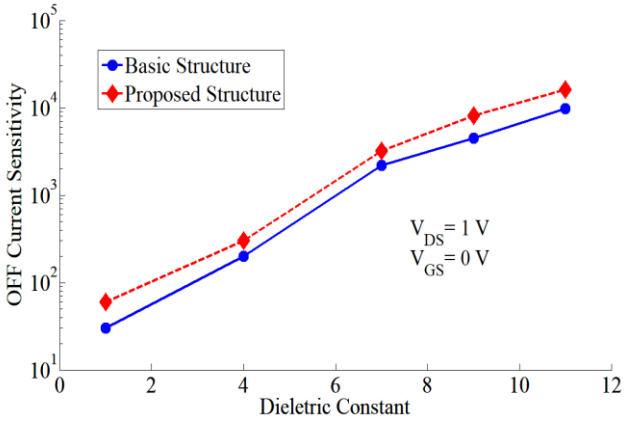

(b)

Fig. 6. The variation in ON and OFF current sensitivities for biomolecules with different dielectric constants for both structures.

Biomolecule presence in cavity region. Fig. 5 illustrates the current sensitivity at different drain source voltages where gate source voltage is fixed at 1 V for both structures. Improvement in current sensitivity is apparent for the proposed structure. To illustrate the results with more clarity, the sensitivities of materials with dielectric constant of $K \leq 4$ have been plotted in Fig. 5 (a) and with dielectric constants of $K > 4$ in Fig. 5 (b). The variation in ON and OFF current sensitivities for biomolecules with different dielectric constants are illustrated in Fig. 6 (a) and (b) for both structures

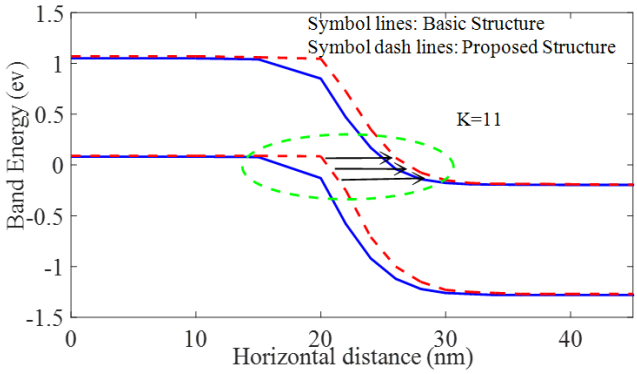

(a)

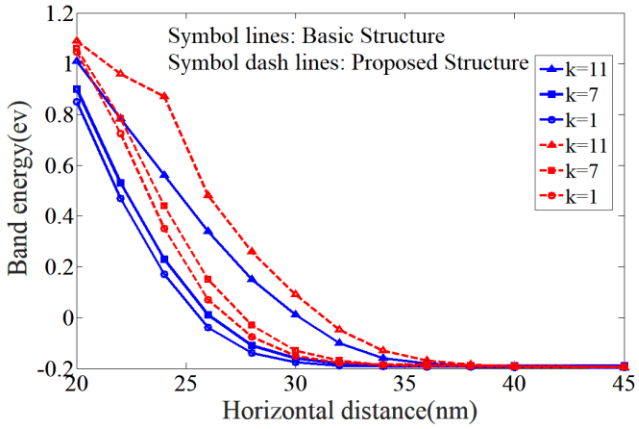

(b)

Fig. 7. (a)The conduction and valance band of both structures for K=1, which shows the higher BTBT for proposed structure and (b) the variations in conduction band at source to channel junction by change in materials in cavity.

The ON state bias is V_{DS}=V_{GS}= 1V, and the OFF state bias is V_{DS}= 1V, V_{GS}= 0V. The result reveals that the proposed structure outperforms the basic counterpart. Fig. 7(a) illustrates the energy band diagram (conduction and valence bands) of the proposed and conventional structure. By increasing the dielectric constant, the band bends significantly. Thus, the threshold voltage decreases, and the saturation current rises. Furthermore, the existence of P^+ region amplifies the BTBT for the proposed biosensor, and consequently, it offers better current characteristics than its conventional counterpart. In Fig. 7(a), the arrows show the horizontal distance between conduction and valance bands of proposed structure. This distance is smaller than its conventional counterpart at source to channel junction, which means the higher BTBT for proposed structure and, consequently, the higher sensitivity. For more clarity, Fig. 7(b) illustrates the change in the conduction band of both structures from source to channel junction to drain region by change in biomolecules in the cavity region. Because of the capacitive behavior of biomolecules, the further band bending is caused by a rising dielectric constant. The presence of P^+ pocket at the source side of TFET causes more changes in the capacitive behavior and current and consequently increases the sensitivity.

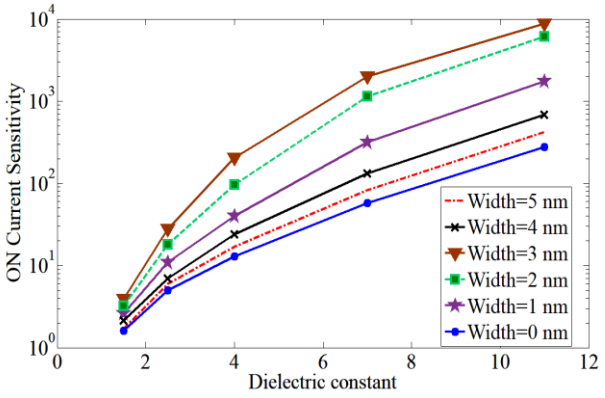

Fig, 8. Variations in sensitivity by the change in width of P^+ pocket where the dielectric constant is varied from 1.5 to 11 and the bias is $V_{DS}=V_{GS}=1$ V and the pocket density is fixed at 5×10^{19} cm^{-3}

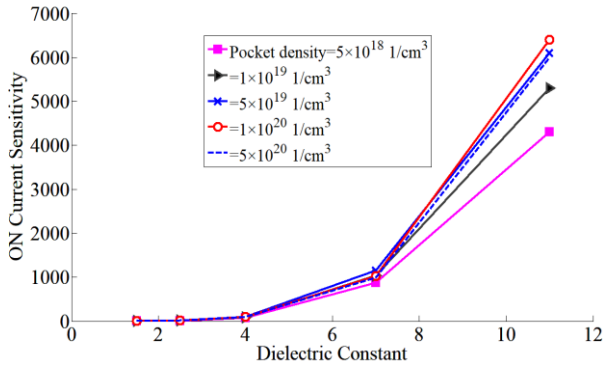

Fig. 9. Variations in sensitivity by the change in density of P^+ pocket where the dielectric constant is varied from 1.5 to 11, the bias is $V_{DS}=V_{GS}=1$ V and the pocket width is fixed at 2 nm.

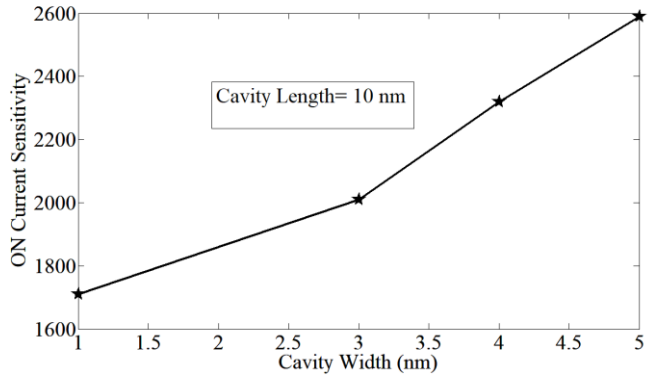

Fig. 10. Variations in sensitivity by the change in cavity width.

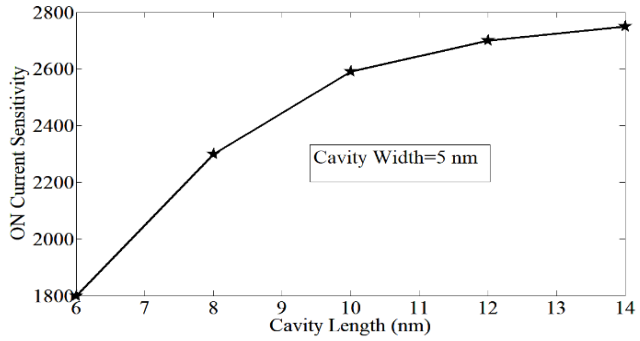

Fig. 11. Variations in sensitivity by the change in cavity length.

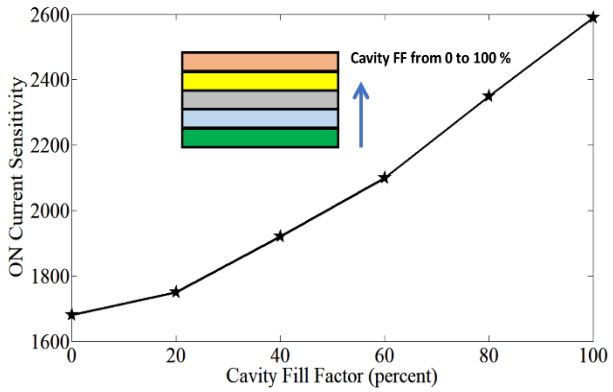

Fig. 12. Variations in sensitivity by the change in cavity fill factor.

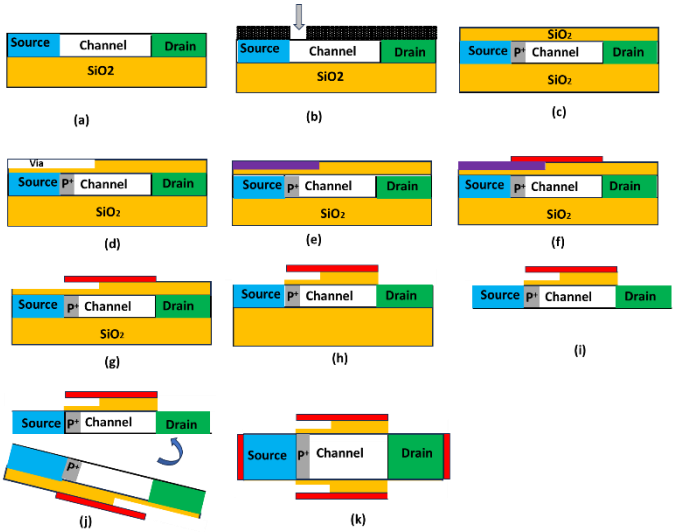

Fig. 13. The schematic view of a sample fabrication process flow of the proposed device.

To investigate the effect of variations in P^+ pocket on sensitivity, we examined different widths for this region, where its density is fixed at 5×10^{19} cm^{-3}. Fig. 8 illustrates the results for W=0, 1, 2, 3, 4, and 5 nm (where W=0 is the conventional structure) at different dielectric constants ranging from 1.5 to 11. It can be seen that the maximum values of sensitivity are obtained where W=3 nm and all widths are larger than the basic structure. Thus, it is possible to choose different widths for the P^+ pocket based on the design demand. Furthermore, it demonstrates the acceptable tolerance for the proposed structure where there are some variations in P^+ pocket width. The designer can choose a 2 or 3 nm width for the pocket region because of their proper values of sensitivity. The proposed device is also examined with different P^+ impurity densities in the pocket region, where the width of the pocket is fixed at 2 nm. Concentrations from 5×10^{18} cm^{-3} to 5×10^{20} cm^{-3} have been investigated, as illustrated in Fig. 9. By increasing the dielectric constant, the difference between the profiles is more obvious. Pocket densities 5×10^{19}, 1×10^{20}, and 5×10^{20} result in proper values for sensitivities, and their values are close to each other. It shows that the designer can choose pocket density among

these values while the sensitivity experiences proper improvement.

Fig.s 10 and 11 investigate the effects of cavity width and length on device sensitivity. It is concluded that by increasing the width and length of the cavity, the sensitivity is improved, resulting from higher effects of the dielectric constant. Fig. 12 shows the results of the fill factor of the cavity on biosensor performance. The more filling cavity, the more sensitivity of biosensor. Furthermore, the device sensitivity is considerably higher than its conventional counterpart, even for a low portion of cavity filling.

The schematic view of a sample fabrication process flow of the proposed device is presented in Fig. 13. A simple silicon on insulator structure with source, channel, and drain regions, which have been created by conventional steps, is used in step (a). The P^+ region is created by ion implantation in step (b). An oxide layer is deposited, followed by via creation in steps (c) and (d). The second oxide is deposited in step (e). The metal layer is created in step (f). The additional oxides on the top and bottom of the structure are etched in steps (g), (h), and (i). Wafer bonding is done in step (j). Finally, the source and drain contacts are created in step (k).

IV. Conclusion

An efficient structure for TFET-based biosensors was proposed in this paper. In conclusion, by using the P^+ pocket in the channel region of TFET, the sensitivity of the biosensor is improved. The energy band diagram is modified at the source side of the channel by embedding a P^+ region. The horizontal distance between the conduction and valance band is reduced, and the probability of BTBT is increased. This issue helps the enhancement in the sensitivity of TFET. Different widths and different impurity concentrations were examined for the pocket region. Also, a wide range of biomolecules with different dielectric constants has been investigated, and the results show that for all investigated materials, the proposed structure enhances the sensitivity where it is more observable for materials with higher dielectric constants. These results demonstrate that the proposed structure is a proper candidate to be used as a TFET biosensor.

REFERENCES

[1] D. Sarkar and K. Banerjee, "Proposal for tunnel-field-effect-transistor as ultra-sensitive and label-free biosensors," *Appl. Phys. Lett*., vol. 100, no. 14, p. 143108, 2012.

[2] D. Sarkar, H. Gossner, W. Hansch, and K. Banerjee, "Tunnel-field-effect transistor-based gas-sensor: Introducing gas detection with a quantum mechanical transducer," *Appl. Phys. Lett*., vol. 102, no. 2, p. 023110, 2013.

[3] R. Narang, M. Saxena, and M. Gupta, "Comparative analysis of dielectric-modulated FET and TFET-based biosensor," *IEEE Trans. Nanotechnol*., vol. 14, no. 3, pp. 427–435, May 2015.

[4] R. Narang, K. V. Sasidhar Reddy, M. Saxena, R. S. Gupta, and M. Gupta, "A dielectric-modulated tunnel-FET-based biosensor for label-free detection: Analytical modeling study and sensitivity analysis." *IEEE trans. Electron devices*, vol.. 59, no. 10, pp. 2809-2817, 2012.

[5] D. Sarkar and K. Banerjee, "Fundamental limitations of conventional FET biosensors: Quantum-mechanical-tunneling to the rescue," *in Proc. IEEE Device Res. Conf.*, pp. 83–84, Jun. 2012.

[6] D. Singh, S. Pandey, K. Nigam, D. Sharma, D. S. Yadav, and P. Kondekar, "A charge-plasma-based dielectric-modulated junctionless TFET for biosensor label-free detection," *IEEE Trans. Electron Devices*, vol. 67, no. 1, pp. 271–278, Jan. 2017.

[7] N. Reddy, N. Nagendra, and D. K. Panda, "A comprehensive review on tunnel field-effect transistor (TFET) based biosensors: recent advances and prospects on device structure and sensitivity." *Silicon* 13, no. 9, pp. 3085-3100, 2021.

[8] R. Narang, K. V. S. Reddy, M. Saxena, R. S. Gupta, and M. Gupta, "A dielectric-modulated tunnel-FET-based biosensor for label-free detection: Analytical modeling study and sensitivity analysis," *IEEE Trans. Electron Devices*, vol.. 59, no. 10, pp. 2809–2817, Oct. 2012.

[9] S. Kanungo, S. Chattopadhyay, P. S. Gupta, K. Sinha, and H. Rahaman, "Study and analysis of the effects of SiGe source and pocket-doped channel on sensing performance of dielectrically modulated tunnel FET-based biosensors," *IEEE Trans. Electron Devices*, vol. 63, no. 6, pp. 2589–2596, Jun. 2016.

[10] A. Bhattacharyya, Ch. Manash, and D. Debashis, "Performance assessment of new dual-pocket vertical heterostructure tunnel FET-based biosensor considering steric hindrance issue", *IEEE Transactions on Electron Devices* 66, no. 9, pp. 3988-3993, 2019.

[11] M. Verma, S. Tirkey, S. Yadav, D. Sharma, D. Yadav, "Performance assessment of a novel vertical dielectrically modulated TFET-based biosensor", *IEEE Transactions on Electron Devices*, vol. 64, no. 9, pp. 3841-3848, 2017.

[12] R. Reddy, D. Panda, "A comprehensive review on tunnel field-effect transistor (TFET) based biosensors: recent advances and prospects on device structure and sensitivity", *Silicon*, vol. 13, no. 9, pp. 3085-3100, 2021.

[13] P. Vimala, L. Krishna, S. Sharma, "TFET Biosensor simulation and analysis for various biomolecules", *Silicon*, vol. 14, no. 13, pp. 7933-7938, 2022.

[14] S. Kumar, Y. Singh, B. Singh, P. K. Tiwari, "Simulation study of dielectric modulated dual channel trench gate TFET-based biosensor", *IEEE Sensors Journal*, vol. 20, no 21, pp. 12565-12573, 2020.

[15] A. Azadi, S. Mohammadi, P. Keshavarzi, "Ion-Sensitive Field-Effect Transistor-Based Biosensor for PSA Antigen Concentration Measurement Using Microfluidic System", *Journal of modeling and simulation in electrical and electronics.* vol. 1, no. 4, pp. 33-36, 2022.

[16] A. Theja, M. Panchore, "Performance investigation of GaSb/Si heterojunction-based gate underlap and overlap vertical TFET biosensor", *IEEE Transactions on NanoBioscience*, vol. 22, no. 2, pp. 284-291, 2022.

[17] K. Vanlalawmpuia, B. Bhowmick, "Analysis of hetero-stacked source TFET and heterostructure vertical TFET as dielectrically modulated label-free biosensors", *IEEE Sensors Journal*, vol. 22, no. 1, pp. 939-947, 2021.

[18] R. Saha, Y. Hirpara, S. Hoque, "Sensitivity analysis on dielectric modulated Ge-source DMDG TFET based label-free biosensor", *IEEE Transactions on Nanotechnology*, vol. 20, pp. 552-560, 2021.

[19] A. Gedam, B. Acharya, G. P. Mishra, "Design and performance assessment of dielectrically modulated nanotube TFET biosensor*", IEEE Sensors Journal*, vol. 21. no. 15, pp.16761-16769, 2019.

[20] S. Das, B. Kumar, P. Bundela, K. Singh, Performance assessment of Si based dual metal double gate vertical TFET biosensor, *Micro and Nanostructures*, vol.. 191, 2024.

[21] K. Baruah, S. Baishya, "Numerical assessment of dielectrically-modulated short-double-gate PNPN TFET-based label-free biosensor", *Microelectronics Journal*, vol. 133, p. 105717, 2023.

[22] J. Bitra, G. Komanapalli, "A comprehensive performance investigation on junction-less tfet (jl-tfet) based biosensor: Device structure and sensitivity", *Transactions on Electrical and Electronic Materials*, vol. 24, no. 5, pp. 365-372, 2023.

[23] S. Panda, S. Dash, "A single gate Si1− xGex dopingless TFET functioned as an effective label-free biosensor", *Physica Scripta*, vol. 98, no. 9, p. 095910, 2023.

[24] M. H. Khan, M. F. Akbar, P. Kaur, G. Wadhwa, "Modeling, simulation investigation of heterojunction (GaSb/Si) vertical TFET-based dielectric modulated biosensor structure", *Micro and Nanostructures*, vol. 179, p. 207565, 2023.

[25] A. Tura, Z. Zhang, P. Liu, Y.-H. Xie, and J. C. S. Woo, "Vertical silicon p-n-p-n tunnel nMOSFET with MBE-grown tunneling junction," *IEEE Trans. Electron Devices*, vol. 58, no. 7, pp. 1907–1913, Jul. 2011.

[26] M. K. Anvarifard, A. A. Orouji, “Design of a novel high-sensitive SOI-Junctionless BioFET overcoming sensitivity degradation problems”, *Scientific Reports*, 14(1), 18395. 2024.
[27] I. C. Cherik, S. Mohammadi, S., A. A. Orouji, “Switching performance enhancement in nanotube double-gate tunneling field-effect transistor with germanium source regions.”, *IEEE Transactions on Electron Devices*, 69(1), 364-369, 2021.
[28] Z. Ramezani, A. A. Orouji, “A new DG nanoscale TFET based on MOSFETs by using source gate electrode: 2D simulation and an analytical potential model”, *Journal of the Korean Physical Society*, *71*, 215-221, 2017.
[29] H. Shahnazarisani, A. A. Orouji, “A novel SOI MESFET by implanted N layer (INL-SOI) for high-performance application”, *Modeling and Simulation in Electrical and Electronics Engineering*, 1(1), 7-12, 2021.
[30] Atlas, device simulator, Atlas user’s manual In: Silvaco international software, Santa Clara, 2015.
[31] D. Djamai, A. Lounis, E. L. Gkougkousis, M. Chahdi, D. Hohov, S. Oussalah, T. Rashid, “Performance of n-on-p planar pixel sensors with active edges at high-luminosity environment”, *The European Physical Journal Plus*, vol. 135, no. 1, p. 101, 2020.
[32] S. Khanjar, A. Naderi, “DC and RF characteristics improvement in SOI-MESFETs by inserting additional SiO2 layers and symmetric Si wells”, *Materials Science and Engineering*: B, vol. 272, p. 115386, 2021.
[33] A. Paliwal, M. Tomar, V. Gupta, “Complex dielectric constant of various biomolecules as a function of wavelength using surface plasmon resonance”, *Journal of Applied Physics*, vol. 116, no. 2, 2014.
[34] A. Densmore, D. Xu, S. Janz, P. Waldron, T. Mischki, G. Lopinski, A. Delâge et al., "Spiral-path high-sensitivity silicon photonic wire molecular sensor with temperature-independent response." *Optics Letters*, vol. 33, no. 6, pp. 596-598, 2008.
[35] E. Makarona, E. Kapetanakis, D. M. Velessiotis, A. Douvas, P. Argitis, P. Normand, T. Gotszalk, M. Woszczyna, and N. Glezos "Vertical devices of self-assembled hybrid organic/inorganic monolayers based on tungsten polyoxometalates", *Microelectronic Engineering*, vol. 85, no. 5-6, pp. 1399-1402, 2008